

## On the First Overtone Spectra of Protonated Water Clusters $[H^+(H_2O)_{3-5}]$ in the Free-OH Stretch Region

C.-C. Wu<sup>a</sup> (吳志哲), C. Chaudhuri<sup>b</sup>, J. C. Jiang<sup>c</sup> (江志強),  
Y. T. Lee<sup>a,b</sup> (李遠哲) and H.-C. Chang<sup>b,\*</sup> (張煥正)

<sup>a</sup>Department of Chemistry, National Taiwan University, Taipei, Taiwan 106, R.O.C.

<sup>b</sup>Institute of Atomic and Molecular Sciences, Academia Sinica, P.O. Box 23-166, Taipei, Taiwan 106, R.O.C.

<sup>c</sup>Department of Chemical Engineering, National Taiwan University of Science and Technology, Taipei, Taiwan 106, R.O.C.

The gas-phase near-infrared spectra of protonated water clusters  $[H^+(H_2O)_n, n = 3 - 5]$  have been obtained using a vibrational predissociation ion trap spectrometer coupled with a tunable optical parametric oscillator laser. The spectral bands in the frequency range from 7000 to 7500  $cm^{-1}$  are assigned to the first overtone vibrations of non-hydrogen-bonded (free) OH stretches. Assignments of the spectra are made with reference to the data for  $H_2O$  vapor,  $(H_2O)_2$  in Ar matrices, and considering the presence of the excess proton in the clusters. Blue shifts of the bands are observed to increase with cluster size and are interpreted in terms of a charge screening effect. The observations have allowed determination of the anharmonicity coefficients of these cluster ions on the basis of the calculations using the term value expression of vibrational energy.

### INTRODUCTION

Overtone spectroscopy is a sensitive probe of the anharmonicity of a chemical bond. For the free water molecule, a large database of overtone transitions has been established for both fundamental understanding of O-H vibrations and atmospheric spectroscopic analyses.<sup>1</sup> In contrast, no overtone spectra of neutral water clusters  $(H_2O)_n$  have yet been observed except that of Ar- $H_2O$ .<sup>2</sup> Recently, studies of global climate changes indicate the importance of overtone spectroscopy of  $(H_2O)_n$ , suggesting that the water dimer (in addition to  $H_2O$ ) is a potential atmospheric absorber of solar radiation<sup>3,4</sup> and the water-nitric acid complex may contribute significantly to atmospheric OH radical production.<sup>4</sup> We have carried out infrared spectroscopic measurements of water-containing cluster ions in our laboratory for several years. As the protonated water cluster  $[H^+(H_2O)_n]$  is one of the most abundant species in the atmosphere,<sup>5</sup> we initiate this overtone study and examine these charged particles in a size-selected manner.

Table 1 gives the first overtone transitions of the pure symmetric stretch ( $2\nu_1$ ), the combination mode of symmetric and asymmetric stretches ( $\nu_1+\nu_3$ ), and the pure asymmetric stretch ( $2\nu_3$ ) of free  $H_2O$ , compiled by Rothman et al.<sup>1</sup> The corresponding data of free  $(H_2O)_n$ , even the simplest dimer, are still lacking. With  $H_2O$  trapped in solid Ar matrices,

Perchard<sup>6</sup> managed to observe the first overtone transitions of the matrix-trapped water dimer at 7151.5  $cm^{-1}$  for  $2\nu_1$ , at 7235.9  $cm^{-1}$  for  $2\nu_3$  (the free-OH stretch), and at 7207.1  $cm^{-1}$  for  $\nu_1+\nu_3$ . Together with the transitions observed in the fundamental and higher overtone regions, harmonic frequencies and anharmonicity coefficients of the water monomer and the dimer trapped in Ar matrices are obtained. The study serves as a useful guide for the search of the overtone transitions of gas-phase water clusters if reasonable matrix-induced frequency shifts of the OH stretches are assumed.

Standard *ab initio* calculations provide a good description of the fundamental vibrations of many clusters and cluster ions,<sup>7</sup> but they fail in predicting the spectra of higher vibrationally excited states. To describe these states, it is imperative to take vibrational anharmonicities into account. Stannard et al.<sup>8</sup> have elaborated on calculations of the overtone/combination spectra of  $XY_2$ -type molecules, focusing on both electrical and mechanical anharmonicities. Using a three-dimensional harmonically coupled anharmonic oscillator model, Kjaergaard et al.<sup>9</sup> calculated the first overtone band intensities of the  $2\nu_1$ ,  $2\nu_3$  and  $\nu_1+\nu_3$  modes of  $H_2O$ . The calculated intensity ratio is about 15:1:50, in good agreement with observations. Polyansky et al.<sup>10</sup> have recently built up a potential energy surface of  $H_2O$  from experimental data and showed that no further significant improvement can be achieved by extending their expression by including higher

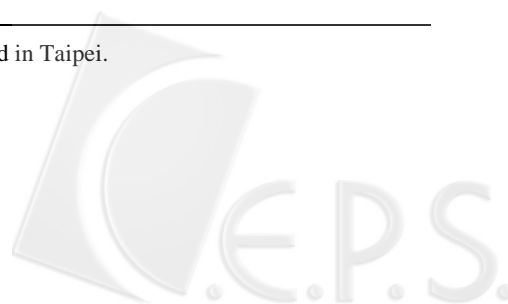


Table 1. Vibrational Frequencies ( $\text{cm}^{-1}$ ) and Assignments of the Observed OH-stretch Absorption Bands of Free Water, the Water Dimer in Ar Matrices, and the Gas-phase Cluster Ions  $\text{H}^+(\text{H}_2\text{O})_{3-5}$ 

Species	Free-OH stretch modes					
	Fundamental			First overtone/combination		
	$\nu_1$	$\nu_f$	$\nu_3$	$2\nu_1$	$2\nu_f$	$\nu_1+\nu_3$
$\text{H}_2\text{O}^{\text{a}}$	3657.1	-	3755.9	7201.5	-	7249.8
$(\text{H}_2\text{O})_2/\text{Ar}^{\text{b}}$	3633.1	3708.0	3737.8	7152	7236	7207.1
$\text{H}^+(\text{H}_2\text{O})_3^{\text{c}}$	3637.4	3667.0	3721.6	7150 (22)	7163 (22)	7190 (15)
$\text{H}^+(\text{H}_2\text{O})_4^{\text{c}}$	3645	-	3731	7174 (12)	-	7216 (14)
$\text{H}^+(\text{H}_2\text{O})_5^{\text{c}}$	3647	3709	3736	7181 (19)	<sup>d</sup>	7224 (18)

<sup>a</sup> Ref. 1.<sup>b</sup> Ar matrix studies (Ref. 6).<sup>c</sup> Fundamental frequencies of  $\nu_1$ ,  $\nu_f$ , and  $\nu_3$  are adapted from Refs. 15-17. Numbers in parentheses denote the bandwidths (full widths at half maxima) obtained from band deconvolution of the spectra in Fig. 2.<sup>d</sup> Not observed.

order terms. The calculations for the fundamental, the first overtone, and their combination bands agree quite well with experiments. To the best of our knowledge, there is no potential energy surface available for water cluster ions (in either protonated or deprotonated forms) in the literature because only very limited experimental term values have been reported so far.

We have conducted in this work near-infrared spectroscopic measurements of protonated water cluster ions [ $\text{H}^+(\text{H}_2\text{O})_n$ ,  $n = 3 - 5$ ] at a cluster temperature around 170 K. Identifications of the observed peaks in the spectra are made with reference to the well-established database of the neutral water monomer and accounting for the charge screening effect in the hydration shell. Since the absorption cross sections of the OH stretches from the first overtone excitations of the cluster ions are much smaller than those from the fundamental excitations (for instance,  $2\nu_1$  is one order of magnitude lower than  $\nu_1$  and  $2\nu_3$  is three orders of magnitude lower than  $\nu_3$  in free  $\text{H}_2\text{O}$ ),<sup>1</sup> the spectroscopic investigation in this field has been a very difficult and challenging task. We present in this communication the first spectroscopic identifications of the first overtone and its combination bands in the near infrared region of small water cluster ions using a home-built vibrational predissociation ion trap spectrometer.

## COMPUTATIONAL AND SPECTROSCOPIC METHODS

Structures and energetics of  $\text{H}^+(\text{H}_2\text{O})_n$ ,  $n = 3 - 5$ , were obtained from density functional theory (DFT) calculations using the commercial GAUSSIAN 98 package.<sup>11</sup> We opti-

mized the geometries of the cluster ions utilizing a standard analytical gradient method without imposing any symmetry constraints at the B3LYP level of computation with the 6-31+G\* basis set (denoted as B3LYP/6-31+G\*). Single-point energy calculations were performed using a larger basis set (aug-cc-pVTZ)<sup>12</sup> for the geometries optimized by the B3LYP/6-31+G level of computation (denoted as B3LYP/aug-cc-pVTZ//6-31+G\*). Table 2 lists the DFT-calculated values of the interaction energies ( $\Delta E_n$ ), the enthalpies ( $\Delta H_n$ ) and the Gibbs free energies ( $\Delta G_n$ ) for the clustering reaction,  $\text{H}^+(\text{H}_2\text{O}) + (n-1)\text{H}_2\text{O} \rightarrow \text{H}^+(\text{H}_2\text{O})_n$ , at 170 and 298 K for various low-energy structures of  $\text{H}^+(\text{H}_2\text{O})_{3-5}$ . The corresponding experimental values of  $\Delta H_n^\circ$  and  $\Delta G_n^\circ$  obtained from the thermochemical measurements<sup>13,14</sup> are given in the same table for comparison. For instance, the total binding enthalpy of  $\text{H}^+(\text{H}_2\text{O})_3$  obtained by Kebarle,<sup>13</sup> Meot-Ner,<sup>14</sup> and their co-workers are 51.1 and 54.0 kcal/mol, respectively, while our B3LYP/aug-cc-pVTZ//6-31+G\* calculation predicts a value of 56.0 kcal/mol after zero-point energy corrections (Table 2). Fig. 1 shows the isomeric structures of  $\text{H}^+(\text{H}_2\text{O})_{3-5}$ , out of which only **HW3I**, **HW4I** and **HW5I** (the lowest-energy isomers of the respective clusters) have been identified in a supersonic expansion in our previous experiments.<sup>15-17</sup>

To obtain the first overtone spectra of the protonated water clusters, experiments were carried out using an ion beam mass spectrometer in conjunction with a pulsed tunable OPO (optical parametric oscillator) laser. Details of the spectrometer have been described elsewhere.<sup>18</sup> The OPO laser (Infinity XPO, Coherent, USA), used for the first time in this experiment, has an output energy of 9 mJ/pulse with a beam diameter of ~5 mm at a repetition rate of 20 Hz when in operation. The laser beam was focused with an  $f = 120$  cm lens into

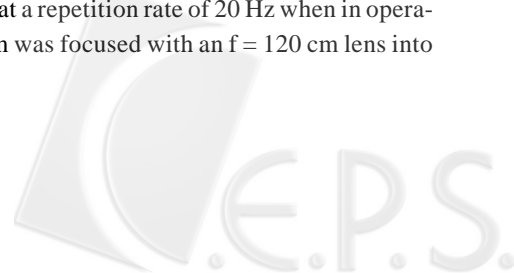


Table 2. Experimental and DFT-calculated Total Energies (kcal/mol) of the Clustering Reaction,  $\text{H}^+(\text{H}_2\text{O}) + (\text{n}-1)\text{H}_2\text{O} \rightarrow \text{H}^+(\text{H}_2\text{O})_n$ , for  $n = 3 - 5$ 

Isomers <sup>a</sup>	Calc. <sup>b</sup>				Expt. <sup>c</sup>	
	$\Delta E_n$	$\Delta H_n^{298}$	$\Delta G_n^{298}$	$\Delta G_n^{170}$	$\Delta H_n^\circ$	$\Delta G_n^\circ$
<b>HW3I</b>	-54.4	-56.0	-39.3	-46.5	-51.1, -54.0	-37.4, -37.9
<b>HW4I</b>	-71.8	-73.9	-49.0	-59.7	-68.6, -71.0	-46.8, -46.0
<b>HW4II</b>	-69.8	-72.0	-47.4	-58.0		
<b>HW4III</b>	-66.6	-69.8	-41.8	-53.8		
<b>HW5I</b>	-83.5	-85.9	-53.3	-67.3	-81.3, -84.0	-52.5, -51.0
<b>HW5II</b>	-80.8	-83.5	-50.6	-64.7		
<b>HW5III</b>	-82.8	-85.8	-50.9	-65.9		

<sup>a</sup> Structures depicted in Fig. 1.

<sup>b</sup> Using B3LYP/aug-cc-pVTZ//6-31+G\* with zero-point vibrational energies corrected.

<sup>c</sup> Refs. 13 and 14.

the laser-cluster interaction region, establishing an estimated energy of  $\sim 5$  mJ/pulse. We calibrated the laser frequency and linewidth with the use of the absorption bands of atmospheric water, obtained by using a Fourier transform infrared spectrometer (MB100, Bomem, Canada) operating in the near-infrared region. The laser is found to have a linewidth of  $\sim 2$   $\text{cm}^{-1}$ .

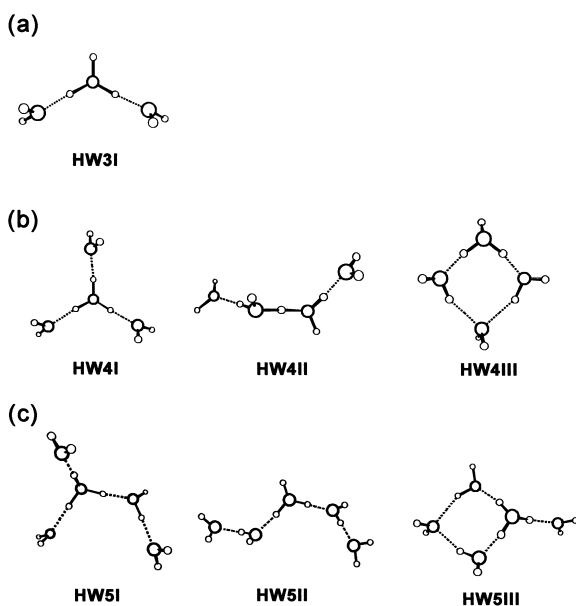


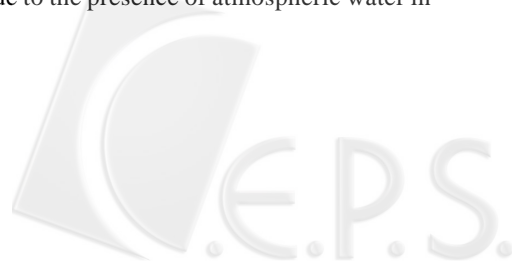
Fig. 1. DFT-optimized geometries of (a)  $\text{H}^+(\text{H}_2\text{O})_3$ , (b)  $\text{H}^+(\text{H}_2\text{O})_4$  and (c)  $\text{H}^+(\text{H}_2\text{O})_5$ . The O and H atoms are denoted by large open and small open circles, respectively. All the structures are optimized with the same level (B3LYP/6-31+G\*) of computation. Isomers **HW3I**, **HW4I**, and **HW5I** have been identified in previous experiments (Refs. 15-17).

We produced the water cluster ions from a supersonic expansion of corona-discharged  $\text{H}_2\text{O}$  vapor seeded in pure  $\text{H}_2$  at a backing pressure of 30-120 Torr behind a room-temperature nozzle. The cluster ions of interest [ $\text{H}^+(\text{H}_2\text{O})_n$ ] were first mass-selected by a  $60^\circ$  sector magnet and stored in an octopole ion trap for both temperature estimation and spectroscopic measurements. The internal temperature of the cluster ions produced under various supersonic conditions typically ranges from 170 to 200 K, as estimated from their self-dissociation rates.<sup>19,20</sup> In performing the spectroscopic measurements, laser photons were introduced into the ion trap to pump the clusters to their second vibrationally excited states. Fragment ions from the water loss channel as a result of the vibrational excitation,  $\text{H}^+(\text{H}_2\text{O})_n + h\nu \rightarrow \text{H}^+(\text{H}_2\text{O})_{n-1} + \text{H}_2\text{O}$ , were selected by a quadrupole mass filter and then collected by a Daly detector. The ion signals were recorded as a function of the excitation laser wavelength to attain the vibrational predissociation spectra. It should be noted that no  $\text{H}^+(\text{H}_2\text{O})_2$  spectra are attainable in the present study because the dissociation energy of  $\text{H}^+(\text{H}_2\text{O})_2$  is higher than the near-infrared single photon energy (20.0-21.5 kcal/mol in the 7000-7500  $\text{cm}^{-1}$  regime) by more than 10 kcal/mol.<sup>13,14</sup>

## RESULTS AND DISCUSSION

### Band assignments

Fig. 2 shows the vibrational predissociation spectra of  $\text{H}^+(\text{H}_2\text{O})_n$  for  $n = 3 - 5$  in the near-infrared region (7000-7500  $\text{cm}^{-1}$ ), along with the percentage transmission of the OPO laser power in the open atmosphere (Fig. 2). Variations of the laser intensity in the scanned frequency range reveal many absorption bands due to the presence of atmospheric water in



the light path between the laser and the spectrometer. Three prominent peaks are found at 7155, 7190 and 7254  $\text{cm}^{-1}$  for  $\text{H}^+(\text{H}_2\text{O})_3$ . Corresponding to the calculated minimum-energy structure **HW3I** (Fig. 1a), the signatures in the spectrum (Fig. 2a) are expected to arise from the symmetric ( $2\nu_1$ ), the dangling free ( $2\nu_f$ ), the asymmetric ( $2\nu_3$ ), and a combination ( $\nu_1+\nu_3$ ) mode of OH stretches in this frequency regime. From the locations of the overtone bands observed for free  $\text{H}_2\text{O}$ , ( $\text{H}_2\text{O})_2$  in Ar matrices (cf. Table 1), and considering the excess positive charge distribution present in the cluster ion, we are led to identification of these overtone bands as discussed below.

According to Rothman et al.,<sup>1</sup> the absorption cross section of  $2\nu_3$  is 17 times smaller than that of  $2\nu_1$  in  $\text{H}_2\text{O}$  vapor, and so the signature of  $2\nu_3$  is not expected to appear in the spectrum. To identify the observed features associated with the three possible vibrations  $2\nu_1$ ,  $2\nu_f$ , and  $\nu_1+\nu_3$ , we notice

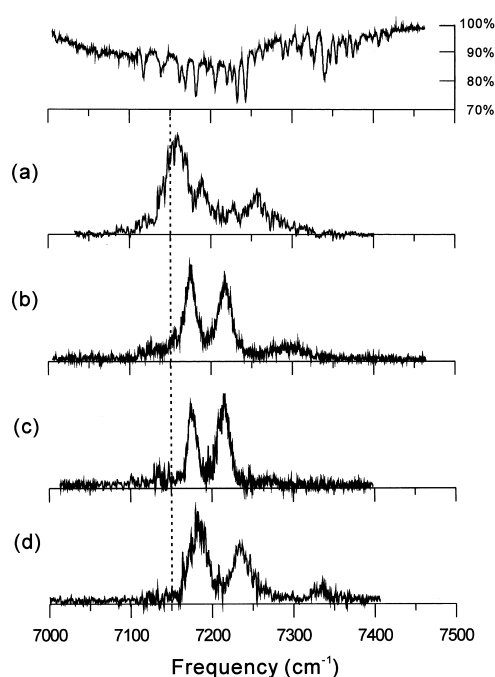


Fig. 2. Power-normalized vibrational predissociation spectra for the first overtone/combination bands of (a)  $\text{H}^+(\text{H}_2\text{O})_3$  at 200 K, (b)  $\text{H}^+(\text{H}_2\text{O})_4$  at 200 K, (c)  $\text{H}^+(\text{H}_2\text{O})_4$  at 170 K, (d)  $\text{H}^+(\text{H}_2\text{O})_5$  at 170 K in the frequency range 7000–7500  $\text{cm}^{-1}$ . The vertical dash line is drawn to indicate the frequency shift of the absorption bands with cluster size. The top curve shows the variation of the OPO laser power intensity due to absorption of atmospheric water, and the scale on the right indicates the percentage transmission of the laser power in the open atmosphere.

that the absorption band at 7155  $\text{cm}^{-1}$  in Fig. 2a is much broader than that of the band at 7190  $\text{cm}^{-1}$  and also the bands standing over almost the same frequency span for  $n = 4$  and 5. A band deconvolution by multi-peak fitting has been thus conducted to resolve this feature into two peaks at 7150 and 7163  $\text{cm}^{-1}$ , as shown by the dotted lines in Fig. 3. The separation of these two peaks ( $\sim 13 \text{ cm}^{-1}$ ) is less than the width (22  $\text{cm}^{-1}$ ) of the individual deconvoluted band. For free  $\text{H}_2\text{O}$ , the pure symmetric, the pure asymmetric, and the combination bands of the first overtone reported by Rothman et al.<sup>1</sup> are located at 7201.5, 7445.1 and 7249.8  $\text{cm}^{-1}$ , respectively. Taking into account the frequency red-shift induced by the charge (i.e.  $\text{H}^+$ ), the presently deconvoluted peaks at 7150 and 7163  $\text{cm}^{-1}$  can be assigned to the first overtone transitions of the symmetric stretch ( $2\nu_1$ ) and the dangling free-OH stretch ( $2\nu_f$ ), whereas the band at 7190  $\text{cm}^{-1}$  can be attributed to the overtone/combination mode of two OH stretches ( $\nu_1+\nu_3$ ), as indicated in Table 1. It is likely that the broad feature at 7254  $\text{cm}^{-1}$ , which is too low to be assigned to  $2\nu_3$ , originates from the first overtone bands of either  $2\nu_1$  or  $\nu_1+\nu_3$  (or both) modes coupled with lower-frequency vibrations of this cluster ion.

Figs. 2b and 2c display the experimental spectra of  $\text{H}^+(\text{H}_2\text{O})_4$  at two different cluster temperatures, 200 and 170 K. The respective spectrum shows two strong absorption bands at 7174 and 7216  $\text{cm}^{-1}$ , and they are ascribable to  $2\nu_1$  and  $\nu_1+\nu_3$  of the four equivalent  $\text{H}_2\text{O}$  molecules of isomer **HW4I** (Fig. 1b). Compared to the spectrum of  $\text{H}^+(\text{H}_2\text{O})_3$ , these two bands are blue-shifted by 24  $\text{cm}^{-1}$  for  $2\nu_1$  and by 26  $\text{cm}^{-1}$  for  $\nu_1+\nu_3$ . Similar to the case of  $\text{H}^+(\text{H}_2\text{O})_4$ , the spectrum of  $\text{H}^+(\text{H}_2\text{O})_5$  at 170 K (Fig. 2d) is dominated by two intense but slightly broader peaks at 7181 and 7224  $\text{cm}^{-1}$  for  $2\nu_1$  and  $\nu_1+\nu_3$ , respectively, of the solvent  $\text{H}_2\text{O}$  molecules. Blue-shifting of both modes by  $\sim 8 \text{ cm}^{-1}$  with respect to those of  $n = 4$  has also occurred (cf. Table 1). For the three cluster ions, no significant change in relative intensity of the  $2\nu_1$  and  $\nu_1+\nu_3$

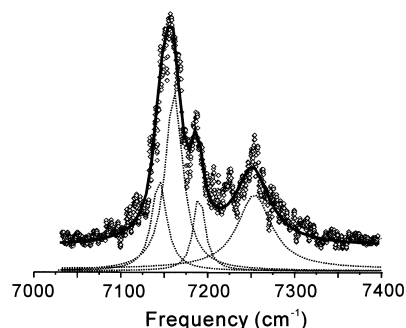


Fig. 3. Deconvolution of the absorption bands of  $\text{H}^+(\text{H}_2\text{O})_3$  in the first overtone free-OH stretch region.

bands in the spectra (Figs. 2a → 2d) is found as the cluster temperature is raised from 170 to 200 K. Furthermore, the bands that are ascribable to the combination modes of  $2\nu_1$  (or  $\nu_1+\nu_3$ ) stretches and low-frequency vibrations can all be identified at  $n = 3 - 5$ .

In contrast to the observation of  $n = 3$ , we failed to detect any absorption feature that can be associated with the free-OH overtone stretch ( $2\nu_f$ ) of  $n = 5$ . We consider that this is because the status of the free O-H of clusters  $n = 3$  and  $5$  are very different from each other; the former belongs to  $\text{H}_3\text{O}^+$  of isomer **HW3**, whereas the later is part of the first-shell  $\text{H}_2\text{O}$  molecule behaving as a single-donor-single-acceptor of isomer **HW5** (Fig. 1). While the  $2\nu_f$  band is not seen at  $n = 5$ , we may estimate where it is located as follows. Since the fundamental free-OH stretch for  $n = 5$  is higher than that for  $n = 3$  by  $42 \text{ cm}^{-1}$  (Table 1), the position of the free-OH overtone band for  $n = 5$  is likely to be found at a frequency higher than  $7163 \text{ cm}^{-1}$ . So considering a difference of  $84 \text{ cm}^{-1}$  in the first overtone region, the  $2\nu_f$  band is expected to peak at around  $7247 \text{ cm}^{-1}$ . From the spectrum displayed in Fig. 2d, it seems that the  $2\nu_f$  band is very weak and either is overlapped with the  $\nu_1 + \nu_3$  mode or it sinks into this broad feature.

### Size-dependent frequency shifts

Red shifts of vibrational frequencies are found in both the fundamental and the first overtone transitions of  $\text{H}^+(\text{H}_2\text{O})_{3-5}$  with respect to those of the neutral water monomer (Table 1). According to Yeh et al.<sup>15</sup> and Crofton et al.,<sup>16</sup> the frequency red-shift of the asymmetric stretch ( $\nu_3$ ) of the cluster ions from that of the monomer ranges from  $34 \text{ cm}^{-1}$  in  $\text{H}^+(\text{H}_2\text{O})_3$  to  $20 \text{ cm}^{-1}$  in  $\text{H}^+(\text{H}_2\text{O})_5$ . For the symmetric stretch ( $\nu_1$ ), the corresponding shift varies from  $20 \text{ cm}^{-1}$  of  $\text{H}^+(\text{H}_2\text{O})_3$  to  $10 \text{ cm}^{-1}$  of  $\text{H}^+(\text{H}_2\text{O})_5$ . These frequency red-shifts are all noticeably smaller than the corresponding shifts in the first overtone region.

In Table 1, an increase in cluster size is seen to give rise to blue shifts of the pure overtone and the overtone/composition bands, analogous to that in the fundamental region. The blue shift for the change in cluster size from  $n = 3$  to  $n = 4$  is about three times larger than that when it goes from  $n = 4$  to  $n = 5$  for  $2\nu_1$ . This difference in blue shift is attributed to two different aspects in stepwise clustering from  $n = 3$  to  $n = 5$ . First, the first solvation shell of the  $\text{H}_3\text{O}^+$  ion is filled as the cluster size increases to  $n = 4$  and, second, the second-shell effect is switched on with further increase of the cluster size to  $n = 5$ . The charge screening effect, where the central ion is surrounded by increasingly more solvent molecules, clearly comes to play upon the second-shell formation at  $n = 5$ . Not

surprisingly, it is the ionic character of the cluster that determines the observed frequency shift.

### Evaluation of anharmonicity coefficients

Theoretical approach for calculating the anharmonicity coefficients from the observed  $G(0,0,0) \rightarrow G(\nu_1, \nu_2, \nu_3)$  overtone transitions of  $\text{H}^+(\text{H}_2\text{O})_{3-5}$  is carried out with help of the fundamental transitions measured by Yeh et al.,<sup>15</sup> Crofton et al.,<sup>16</sup> and Jiang et al.<sup>17</sup> (Table 1), along with the overtone/composition bands observed in this work using the quantum mechanical term value equations of vibrational energy.<sup>21</sup> Determination of the anharmonicity coefficients requires a preliminary analysis of cluster structure. In Table 2, the B3LYP/aug-cc-pVTZ//6-31+G\* calculations predict that the lowest-energy isomers of the cluster ions  $\text{H}^+(\text{H}_2\text{O})_4$  and  $\text{H}^+(\text{H}_2\text{O})_5$  are more stable than the corresponding second-lowest energy isomers by  $\Delta(\Delta G_n^{170}) = 1.7$  and  $1.4 \text{ kcal/mol}$ , respectively. Previously,<sup>15-17</sup> we have experimentally identified isomers **HW3I**, **HW4I**, **HW5I** (Fig. 1) for these gas-phase ions in the temperature range from 170 to 200 K. In this work, with similar ion-beam conditions, we rule out the possibility for the existence of other isomers in the supersonic expansion and so the observed overtone spectra should be mainly contributed from the isomers **HW3I**, **HW4I**, **HW5I**. Once the problem of structural identification is solved, the anharmonicity coefficients  $x_{ij}$  and the harmonic frequencies  $\omega_i$  appearing in the quantum mechanical term value expression of vibrational energy can be evaluated:<sup>21</sup>

$$G(\nu_1, \nu_2, \nu_3) = \sum_{i=1}^3 \omega_i (\nu_i + \frac{1}{2}) + \sum_{i,j=1, i \neq j}^3 x_{ij} (\nu_i + \frac{1}{2})(\nu_j + \frac{1}{2}) + \dots \quad (1)$$

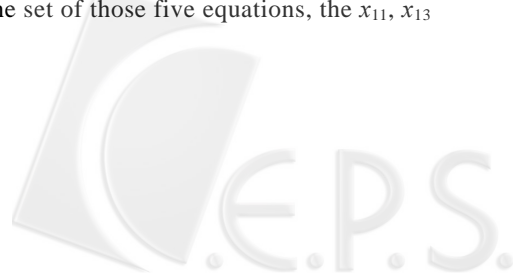
where  $\omega_i$  and  $x_{ij}$  are in  $\text{cm}^{-1}$  and  $\nu_i$  ( $\nu_1 =$  symmetric stretch,  $\nu_2 =$  bending,  $\nu_3 =$  asymmetric stretch) are the vibrational quantum numbers. From eqn. (1), we have

$$\begin{aligned} G_0(\nu_1, \nu_2, \nu_3) &= G(\nu_1, \nu_2, \nu_3) - G(0,0,0) \\ &= \sum_{i=1}^3 \omega_i^0 \nu_i + \sum_{i,j=1, i \neq j}^3 x_{ij}^0 \nu_i \nu_j + \dots, \end{aligned} \quad (2)$$

where

$$\omega_i^0 = \omega_i + x_{ii} + \frac{1}{2} \sum_{i \neq j}^3 x_{ij} + \dots, \quad (3)$$

and  $x_{ij}^0 = x_{ij}$  when higher order terms are neglected. Now, a set of five equations can be derived from eqn. (2) with  $G_0(1,0,0)$ ,  $G_0(0,0,1)$ ,  $G_0(2,0,0)$ ,  $G_0(1,0,1)$  and  $G_0(0,0,2)$ , and there are five anharmonicity coefficients  $x_{11}$ ,  $x_{12}$ ,  $x_{13}$ ,  $x_{23}$ , and  $x_{33}$  to be evaluated. Using the set of those five equations, the  $x_{11}$ ,  $x_{13}$





and  $x_{33}$  can be expressed as

$$x_{11} = [G_0(2,0,0) - 2G_0(1,0,0)]/2 \quad (4)$$

$$x_{13} = G_0(1,0,1) - [G_0(1,0,0) + G_0(0,0,1)] \quad (5)$$

$$x_{33} = [G_0(0,0,2) - 2G_0(0,0,1)]/2 \quad (6)$$

Since we have not yet observed the  $2\nu_3$  band, i.e.  $G_0(0,0,2)$ , we can calculate only  $x_{11}$  and  $x_{13}$  out of the five coefficients. Placing the values of the observed frequencies for the fundamental and the overtone/combination bands from Table 1 in eqns. (4) and (5), we obtain the values of  $x_{11}$  and  $x_{13}$ , and the vibrational constant ( $\omega_1^0$ ) from the relation [ $\omega_1^0 = G_0(1,0,0) - x_{11}$ ]<sup>21</sup> for all three cluster ions  $H^+(H_2O)_{3-5}$ , as given in Table 3.

We note that the anharmonicity coefficients  $x_{11}$  and  $x_{13}$  in Table 3 show a discrete change from  $H^+(H_2O)_3$  to  $H^+(H_2O)_4$ , but these terms for  $H^+(H_2O)_4$  and  $H^+(H_2O)_5$  reach almost the same value. From a structural analysis of  $H^+(H_2O)_3$  (Fig. 1), the isomer **HW3I** contains a hydronium ion core bound to two water molecules with  $C_{2v}$  symmetry. Addition of another water molecule to it fills up the first solvation shell, yielding the minimum-energy isomer **HW4I**. Completion of the first solvation shell clearly makes the anharmonicity to reach a steady value for  $n = 4$  and 5. These characters of discrete change from  $H^+(H_2O)_3$  to  $H^+(H_2O)_4$  are also found in the blue shifts of vibrational frequencies (Table 1) and in the thermochemical measurements of dissociation energies (Table 2).

## CONCLUSION

We have chosen the most fundamental cluster ions, the protonated water clusters [ $H^+(H_2O)_n$ ,  $n = 3 - 5$ ], as the candidate for spectroscopic studies in the near-infrared region (7000-7500  $cm^{-1}$ ). The study presents the first step toward exploration of the mystic region of hydrogen-bonded cluster ions by photo-excitation to the first overtone level of OH stretching modes and inducing vibrational predissociation.

Table 3. Harmonic Frequencies ( $cm^{-1}$ ) and Anharmonicity Coefficients ( $cm^{-1}$ ) of the Free-OH Stretches of  $H_2O$  and  $H^+(H_2O)_{3-5}$  Extracted from Experimental Values Using the Term Value Expression of Vibrational Energy<sup>a</sup>

	$\omega_1^0$	$x_{11}$	$x_{13}$
$H_2O^b$	3693.8	-43.8	-155.0
$H^+(H_2O)_3$	3699	-62	-169
$H^+(H_2O)_4$	3703	-58	-160
$H^+(H_2O)_5$	3703	-56	-159

<sup>a</sup> See eqns. (4) and (5) in text.

<sup>b</sup> Ref. 1.

We have identified two pure overtone bands  $2\nu_1$  and  $2\nu_2$ , and a combination band  $\nu_1 + \nu_3$ . A blue shift is observed for each absorption band as the cluster size increases from  $n = 3$  to  $n = 5$ . Direct comparison of the fundamental and the first overtone band positions clearly shows how the anharmonicity of the free OH stretching is correlated with cluster size. With the help of model calculation of the term value of vibrational energy, two anharmonicity coefficients have been deduced. The data should help to calibrate the results from computer simulations and may also serve to map out the potential surfaces and the interaction modes at a quantum state-to-state level. This work represents the first spectroscopic study in the near-infrared region to observe the first overtone bands of water-containing cluster ions and we expect to obtain more information in the future.

## ACKNOWLEDGEMENTS

We thank the Academia Sinica and the National Science Council (Grant No. NSC 90-2113-M-001-043) of Taiwan, Republic of China, for financial support of this work.

Received July 9, 2002.

## Key Words

Overtone spectroscopy; Protonated water clusters.

## REFERENCES

- Rothman, L. S.; Gamache, R. R.; Tipping, R. H.; Rinsland, C. P.; Smith, M. A. H.; Benner, D. C.; Devi, V. M.; Flaud, J.-M.; Camy-Peyret, C.; Perrin, A.; Goldman, A.; Massie, S. T.; Brown, L. R.; Toth, R. A. *J. Quant. Spectrosc. Radiat. Transfer* **1992**, *48*, 469.
- Plusquellic, D. F.; Votava, O.; Nesbitt, D. J. *J. Chem. Phys.* **1994**, *101*, 6356. Votava, O.; Fair, J. R.; Plusquellic, D. F.; Riedle, E.; Nesbitt, D. J. *J. Chem. Phys.* **1997**, *107*, 8854.
- Chýlek, P.; Geldart, J. W. *Geophys. Res. Lett.* **1997**, *24*, 2015. Tso, H. C. W.; Geldart, J. W.; Chýlek, P. *J. Chem. Phys.* **1998**, *108*, 5319.
- Low, G. R.; Kjaergaard, H. G. *J. Chem. Phys.* **1999**, *110*, 9104. Kjaergaard, H. G. *J. Phys. Chem. A* **2002**, *106*, 2979.
- Wayne, R. P. *Chemistry of Atmospheres*; Oxford University Press: Oxford, 1991.
- Perchard, J. P. *Chem. Phys.* **2001**, *273*, 217.
- Jiang, J. C.; Chang, J.-C.; Wang, B.-C.; Lin, S. H.; Lee, Y. T.; Chang, H.-C. *Chem. Phys. Lett.* **1998**, *289*, 373 and references therein.



8. Stannard, P. R.; Elert, M. L.; Gelbart, W. M. *J. Chem. Phys.* **1981**, *74*, 6050.
9. Kjaergaard, H. G.; Henry, B. R.; Wei, H.; Lefebvre, S.; Carrington, T.; Mortensen, O. S.; Sage, M. L. *J. Chem. Phys.* **1994**, *100*, 6228.
10. Polyansky, O. L.; Jensen, P.; Tennyson, J. *J. Chem. Phys.* **1996**, *105*, 6490.
11. Gaussian 98, Revision A.5, Frisch, M. J.; Trucks, G. W.; Schlegel, H. B.; Scuseria, G. E.; Robb, M. A.; Cheeseman, J. R.; Zakrzewski, V. G.; Montgomery, Jr., J. A.; Stratmann, R. E.; Burant, J. C.; Dapprich, S.; Millam, J. M.; Daniels, A. D.; Kudin, K. N.; Strain, M. C.; Farkas, O.; Tomasi, J.; Barone, V.; Cossi, M.; Cammi, R.; Mennucci, B.; Pomelli, C.; Adamo, C.; Clifford, S.; Ochterski, J.; Petersson, G. A.; Ayala, P. Y.; Cui, Q.; Morokuma, K.; Malick, D. K.; Rabuck, A. D.; Raghavachari, K.; Foresman, J. B.; Cioslowski, J.; Ortiz, J. V.; Stefanov, B. B.; Liu, G.; Liashenko, A.; Piskorz, P.; Komaromi, I.; Gomperts, R.; Martin, R. L.; Fox, D. J.; Keith, T.; Al-Laham, M. A.; Peng, C. Y.; Nanayakkara, A.; Gonzalez, C.; Challacombe, M.; Gill, P. M. W.; Johnson, B.; Chen, W.; Wong, M. W.; Andres, J. L.; Gonzalez, C.; Head-Gordon, M.; Replogle, E. S.; Pople, J. A. Gaussian, Inc., Pittsburgh, PA, 1998.
12. Xantheas, S. S. *J. Chem. Phys.* **1995**, *102*, 4505.
13. Lau, Y. K.; Ikuta, S.; Kebarle, P. *J. Am. Chem. Soc.* **1982**, *104*, 1462.
14. Meot-Ner, M.; Speller, C. V. *J. Phys. Chem.* **1986**, *90*, 6616.
15. Yeh, L. I.; Okamura, M.; Myers, J. D.; Price, J. M.; Lee, Y. T. *J. Chem. Phys.* **1989**, *91*, 7319.
16. Crofton, M. W.; Price, J. M.; Lee, Y. T. in *Clusters of Atoms and Molecules*; Haberland, H. ed.; Springer Verlag: Berlin, 1994, Vol. II. p. 44. Price, J. M. Ph.D. Thesis, University of California at Berkeley, 1990.
17. Jiang, J. C.; Wang, Y.-S.; Chang, H.-C.; Lin, S. H.; Lee, Y. T.; Niedner-Schatteburg, G.; Chang, H.-C. *J. Am. Chem. Soc.* **2000**, *122*, 1398.
18. Wang, Y.-S.; Chang, H.-C.; Jiang, J. C.; Lin, S. H.; Lee, Y. T.; Chang, H.-C. *J. Am. Chem. Soc.* **1998**, *120*, 8777.
19. Klots, C. E. *Z. Phys. D* **1991**, *20*, 105.
20. Ichihashi, M.; Yamabe, J.; Murai, K.; Nonose, S.; Hirao, K.; Kondow, T. *J. Phys. Chem.* **1996**, *100*, 10050.
21. Herzberg, G. *Molecular Spectra and Molecular Structure II. Infrared and Raman Spectra of Polyatomic Molecules*; Van Nostrand, New York, 1944, Chapter III, pp. 281.

